

Ion implantation with scanning probe alignment

A. Persaud,^{a)} J. A. Liddle, and T. Schenkel^{b)}

E. O. Lawrence Berkeley National Laboratory, Berkeley, California 94720

J. Bokor

E. O. Lawrence Berkeley National Laboratory, and Department of Electrical Engineering and Computer Science, University of California, Berkeley, California 94720

Tzv. Ivanov and I. W. Rangelow

Institute of Microstructure Technologies and Analytics, University of Kassel, Kassel, Germany

(Received 3 June 2005; accepted 8 August 2005; published 2 December 2005)

We describe a scanning probe instrument which integrates ion beams with the imaging and alignment function of a piezoresistive scanning probe in high vacuum. The beam passes through several apertures and is finally collimated by a hole in the cantilever of the scanning probe. The ion beam spot size is limited by the size of the last aperture. Highly charged ions are used to show hits of single ions in resist, and we discuss the issues for implantation of single ions. © 2005 American Vacuum Society. [DOI: 10.1116/1.2062628]

I. INTRODUCTION

There is a wide range of applications for local modification of surfaces with scanning probes,¹ and deposition of metal lines through nanostencils.^{2,3}

Our setup combines ion beams with scanning probes.⁴ Due to the ion sources used, we can implant a wide spectrum of ions species with variable energy at precise locations into target materials. The alignment resolution is given by the integrated scanning probe and is currently of the order of 5 nm.⁴ The size of the implanted area is given by the size of the last aperture, and a technique for formation of 5 nm holes in scanning probe tips has been demonstrated.⁵

The advantage of this setup is that small areas can be implanted with very precise alignment and with noninvasive imaging of the area of interest. In particular for low dose or in the extreme case of single ion implantation this is a crucial requirement. This is in contrast to focused ion beam (FIB) systems, where the ion beam has to be aligned with an electron beam outside the region of interest to avoid implantation during imaging. Furthermore, low ion intensities needed for low dose implantation in a FIB require fast chopping and low beam intensities which can adversely affect beam quality and increase the difficulty of alignment imaging.

II. EXPERIMENT

A. Setup

Our setup utilizes two ion sources. A medium current source, which produces low energy, low charge state ions and an electron beam ion trap (EBIT). The latter produces a low emittance ($\leq 0.2\pi$ -mm-mrad), low current beam of highly charged ions (HCIs).⁶ The ions are transported to a bending magnet where we can select a specific charge state. In the experiments described here, we use our medium cur-

rent source to produce nA of Ar²⁺ ions with a beam energy of 6 keV and the EBIT to produce pA of Xe³⁰⁺ (195 keV) and Bi⁴⁵⁺ (120 keV). Figure 1 shows a magnet scan of Bi⁹⁺ ions extracted from the EBIT. The EBIT was operated in leaky mode where ionization potential and extraction potential equaled 3.5 kV. Bismuth is supplied to the ion source from an oven. Typical ion intensities are 10⁷ ions/(mm² s). The experimental setup is shown schematically in Fig. 2.

The target is mounted on a nanometer positioning stage which has a range of 100 $\mu\text{m} \times 100 \mu\text{m} \times 10 \mu\text{m}$. The last lens element of the beamline is positioned several mm above the target surface, and the cantilever is positioned inbetween. During scans the cantilever is held in a fixed position and the stage is moved to acquire the scan image. For coarse motion and alignment the cantilever itself is mounted on a flexure stage and can be positioned freely over the region of interest. The flexure stage is also used to achieve the coarse approach of the tip to the surface.

B. Scanning probe

We use a piezoresistive readout scheme to sense the deflection of the cantilever when imaging the target surface. The cantilevers have a Wheatstone bridge built in^{7,8} and a vacuum preamplifier ($\times 10$) integrated close to the cantilever. A second amplification stage ($\times 10 - \times 5000$) outside the vacuum is used in combination with a low pass filter before the signal is fed into the control hardware for the feedback loop.

For imaging we use tips produced by Pt deposition with a dual beam FIB⁸ or glued on commercial tips. For the latter the beam of a commercially available cantilever is broken off and glued onto the piezoresistive cantilever. An example from this technique is shown in Fig. 3. Figure 4 shows an in situ image of a test sample with 50 nm wide trenches taken with the scanning probe.

Holes are drilled into cantilevers in a FIB with a 30 keV Ga⁺ beam. These micron sized holes can then be reduced in

^{a)} Author to whom correspondence should be addressed; electronic mail: apersaud@lbl.gov

^{b)} Electronic mail: t_schenkel@lbl.gov; www: <http://ebit.lbl.gov>

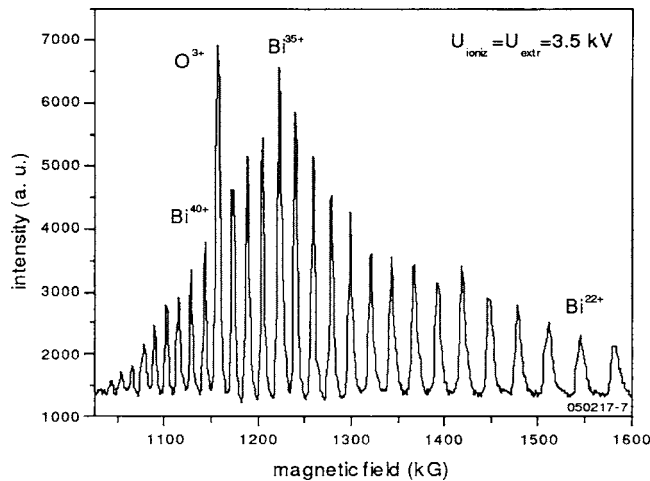


FIG. 1. Magnet scan of a Bismuth beam at an extraction energy of 3.5 keV.

diameter by ion beam assisted deposition of platinum or SiO_2 . Figure 3 shows a glued on tip with three holes of different sizes drilled into it. The insert shows a hole with a diameter of 100 nm, reduced from the initial micron size by deposition of SiO_2 .

III. RESULTS AND DISCUSSION

To test the implantation through the holes in the cantilever we use Si wafers coated with poly(methyl methacrylate) (PMMA) resist and expose the resist with the ion beam. The PMMA we use has a molecular weight of 950 k and the film thickness was 35 nm. After exposure the samples are developed in a 1:3 MIBK:IPA solution for 1 min. Results from Ar exposure (dose $\sim 10^{13}$ ions/cm²) are shown in Fig. 5. In comparison to results reported earlier,⁴ we were able to improve the beam quality of our medium current ion source by additional collimation of the beam, which resulted in undistorted holes following transmission of 500 nm wide, round holes in the cantilever.

HCIs are a very desirable choice for implantation of single ions, because HCIs not only deposit kinetic energy in the material but also large amounts of potential energy (the

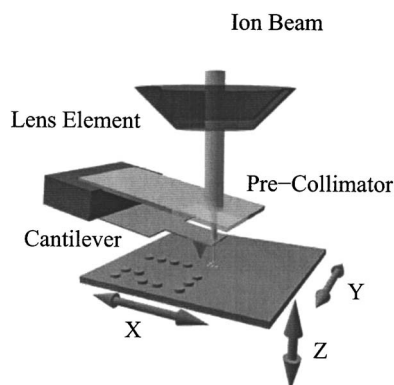


FIG. 2. Schematic of the setup. The beam passes from the last lens through the hole drilled in the cantilever. The cantilever can be positioned anywhere relative to markers on the sample. A precollimator can be mounted on the cantilever to only allow ions through the hole in the cantilever.

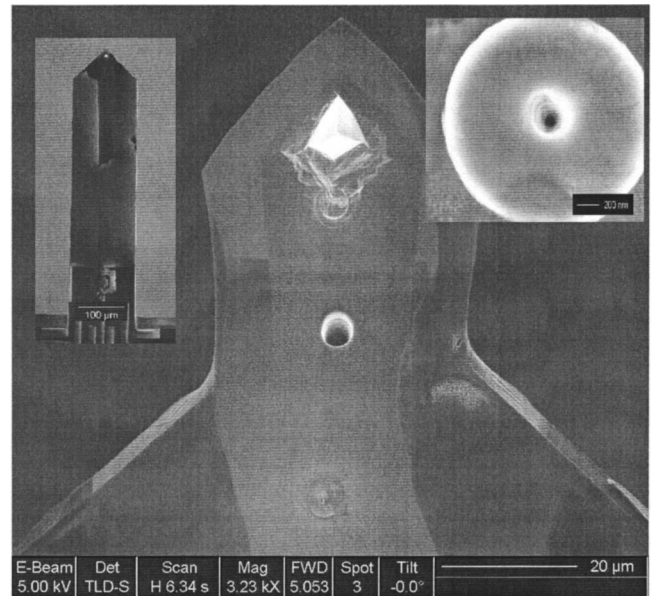


FIG. 3. FIB processed tip. Three holes of different sizes ranging from 1 μm to 100 nm have been drilled through the cantilever. Left inset shows the whole cantilever with the Wheatstone bridge at the bottom, the right inset shows a blow up of the upper 100 nm hole.

sum of the binding energies of the removed electrons). This extra energy results in an increased production of secondary electrons on impact⁹ and also in the creation of more electron/hole pairs inside the material,¹⁰ which can make detection of low energy, single ions easier, compared to detection of single charged ions.¹¹ The potential energy is also independent of the kinetic energy and therefore especially shallow implants benefit from HCIs. In Fig. 6 Bi^{45+} ($E_{\text{pot}} = 37$ keV) were implanted into PMMA and single ion hits can be seen due to the enhanced resist development power of

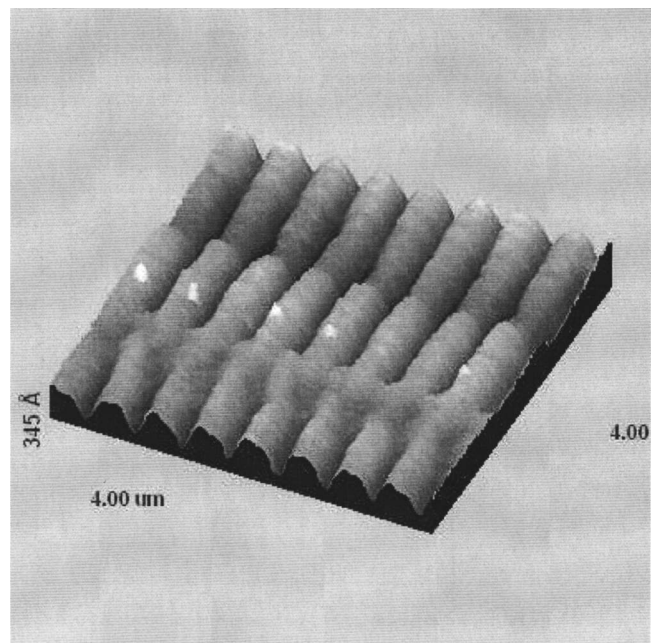


FIG. 4. In situ image of a test sample with 250 nm linewidth and 50 nm wide trenches.

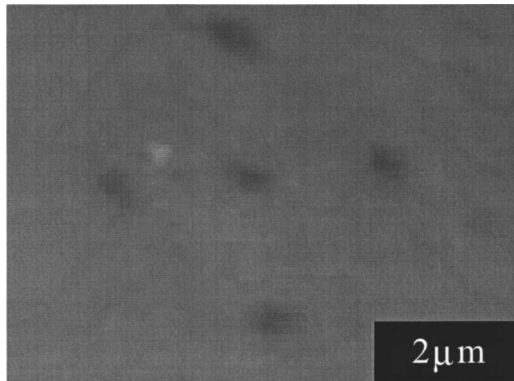


FIG. 5. Array of holes formed with Ar^{2+} exposure in PMMA resist. The resist was exposed for 20 s with a beam current of 1 nA/mm².

HCl.¹² The ions were implanted through a 2 μm wide hole in a cantilever. A single ion crater from the impact of a Bi^{45+} ion shows a diameter of 50 nm. This dopant atom is now aligned to this hole in the resist, enabling formation of a device for probing single atom effects.

Registration of single ion impacts via detection of secondary electrons requires efficient collection of secondary electrons from ion hits on the target in the electron collector, while collection of secondary electrons emitted from collimating apertures has to be suppressed. Efficient detection (>90%) of P^{13+} and Te^{33+} ions has been demonstrated without the scanning probe alignment,⁹ but collection efficiency for secondary electrons emitted from the surface were found to be reduced with the integration of the scanning probe. Figure 7 shows pulse height spectra of secondary electrons collected following the impact of Bi^{45+} ions on silicon targets. The mean pulse height is reduced when the scanning

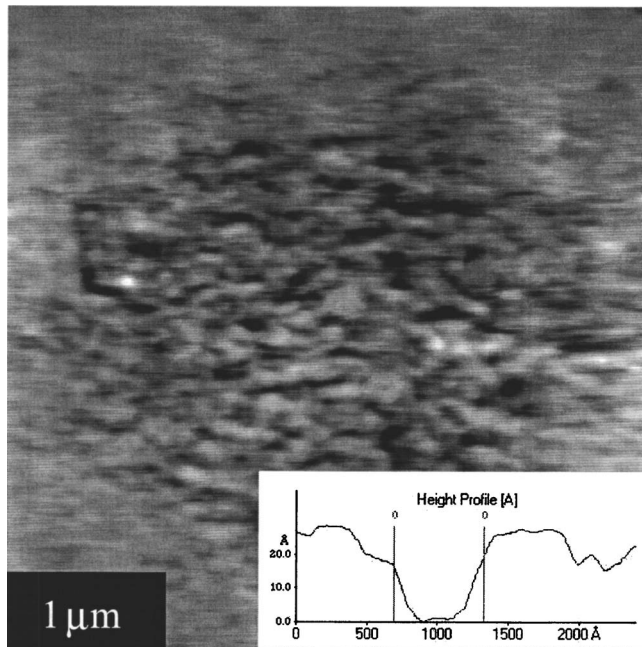


FIG. 6. Craters formed by impacts of single HCIs in PMMA. The inset shows a line out of a single ion hit.

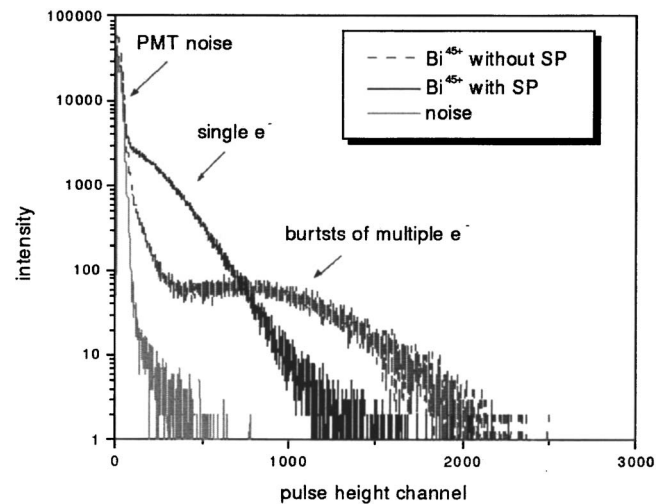


FIG. 7. Pulse height spectrum of secondary electron emission from HCIs with the scanning probe in place.

probe is inserted, indicating that fewer electrons reach the detector following hits on the top side of the cantilever, as compared to hits on the target. For demonstrations of single ion placement suppression of electrons from collimating apertures, and collection of electrons from true target hits have to be improved.

IV. SUMMARY AND OUTLOOK

Our setup for aligned ion implantation using a scanning probe has been presented. The resolution is limited by the hole size of the smallest aperture, currently 100 nm, and experiments with smaller holes are in progress. For small hole sizes the straggling (e.g., ~5 nm for 50 keV Bi ions in silicon) of the ions during implantation will be of the same order of magnitude as the diameter of the hole and thus a resolution of about 5 nm for single ion placement seems possible.

ACKNOWLEDGMENTS

The authors thank the staffs of the UC Berkeley Microlab and the National Center for Electron Microscopy at LBNL for their support and Sunghoon Kwon for the test samples. This work was supported by NSA under ARO Contract No. MOD707501, and by the U.S. DOE under Contract No. DE-AC03-76SF00098.

¹A. A. Tseng, A. Notargiacomo, and T. P. Chen, *J. Vac. Sci. Technol. B* **23**, 877 (2005).

²R. Lüthi *et al.*, *Appl. Phys. Lett.* **75**, 1314 (1999).

³S. Egger *et al.*, *Nano Lett.* **5**, 15 (2005).

⁴A. Persaud *et al.*, *Nano Lett.* **5**, 1087 (2005).

⁵T. Schenkel *et al.*, *J. Vac. Sci. Technol. B* **21**, 2720 (2003).

⁶T. Schenkel *et al.*, *Rev. Sci. Instrum.* **73**, 663 (2002).

⁷I. W. Rangelow *et al.*, *Proc. SPIE* **2879**, 56 (1996).

⁸A. Persaud *et al.*, *J. Vac. Sci. Technol. B* **22**, 2992 (2004).

⁹A. Persaud *et al.*, *Quantum Inf. Process.* **3**, 233 (2004); S. J. Park *et al.*, *Microelectron. Eng.* **73–74**, 695 (2004).

¹⁰T. Schenkel *et al.*, *Phys. Rev. Lett.* **83**, 4273 (1999).

¹¹D. Jamieson *et al.*, *Appl. Phys. Lett.* **86**, 202101 (2005).

¹²T. Schenkel *et al.*, *J. Vac. Sci. Technol. B* **16**, 3298 (1998).